ELSEVIER

Chemical Geology 229 (2006) 28–41

CHEMICAL GEOLOGY
INCLUDING
ISOTOPE GEOSCIENCE

www.elsevier.com/locate/chemgeo

Viscosity, structure and mixing in (Ca, Na) silicate melts

Daniel R. Neuville

Physique des Minéraux et des Magmas, CNRS, Institut de Physique du Globe de Paris, 4 place Jussieu, 75252 Paris Cedex 05, France

Accepted 6 January 2006

Abstract

Configurational entropy has been linked with the structure of Na_2O–CaO–SiO_2 melts, based on combined viscosimetry and Raman spectroscopic investigations. From viscosity measurements at low and high temperatures, we have obtained the configurational entropy, S^{conf} (using $\log \eta = A_e + B_e / TS^{conf}$, where η is the viscosity, T the temperature and A_e, B_e two constants). Using Raman spectroscopy, we obtained structural information from the Q speciation and from the variation of the boson peak with chemical composition.

A rapid decrease in the viscosity at low temperature was observed in Ca-silicate melts with addition of Na_2O. At high temperature, the viscosity is almost the same for the Ca- and Na-silicate liquids. The configurational entropy calculated from the viscosity measurements for Ca/Na mixing shows a non-ideal variation, which can be interpreted in term of non-random distribution of Na and Ca in the silicate network. The addition of Na_2O to the Ca-silicate melts produces a decrease of the fragility of the liquid and an increase of the Q^3/Q^2 ratio observed with Raman spectroscopy.

Keywords: Silicate; Viscosity; Structure; Soda-time melts

1. Introduction

The relationships between physical properties and structure of glasses and melts in the system Na_2O–CaO–SiO_2 are technologically and geologically important, in particular to understand the microscopic origin of the configurational thermodynamic properties. Geologically, this system contains one of the major alkali and alkaline-earth elements found in igneous rocks. The connection of these elements with the tetrahedral silicate network is fundamental to understand the physical properties of magmatic liquids. This system is also technologically important since it represents nearly 80% of industrial glasses and in particular, soda–lime silica glasses are the basis of conventional windows (Morey and Bowen, 1925) and container glasses, as well as bioactive glasses (Hench, 1991; Kim et al., 1995; Clupper and Hench, 2003). This system has been one of the most studied during the last century. The first works on this system were carried out by Morey and Bowen (1925) and Wyckoff and Morey (1925), who published melting relations together with X-ray diffraction patterns of crystalline phases. English (1923) published viscosity measurements between 970 K and 1670 K for glasses with high silica content belonging to this system.

Despite the importance of this system, the majority of measurements were made at high content of silica (65 and 70 mol%) because of the high hygroscopicity of compositions with lower silica content (English, 1923; Gehlgoff and Thomas, 1926; Boow et al., 1942). Unfortunately, glass compositions with more

E-mail address: neuville@ipgp.jussieu.fr.

0009-2541/$ - see front matter © 2006 Elsevier B.V. All rights reserved.
doi:10.1016/j.chemgeo.2006.01.008

than 65% of SiO_2 present an unmixing zone for lime silicate compositions (Morey and Bowen, 1925) and total Ca/Na substitution cannot be made and studied. Compilations of viscosity were made by Mazurin et al. (1987), and Bansal and Doremus (1986) and Kozyukov and Mazurin (1994) have published an empirical model to predict the viscosity for glasses in the Na_2O–CaO–SiO_2 system, which gives good results for glasses with more than 70 mol% of SiO_2.

In this paper, we focus first on viscosity measurements on compositions with lower amounts of silica, 60 mol%, for which a complete Ca/Na substitution is possible. With these new viscosity data and using the theory of relaxation processes of Adam and Gibbs (1965), the viscosity (η) can be linked to the configurational entropy of the liquid (S^{conf}) at temperature T, using the equation proposed by Richet (1984):

$$\log\eta = A_e + B_e/TS^{conf}(T), \quad (1)$$

where T is the temperature, A_e a pre-exponential factor and B_e a measure of the Gibbs-free energy barriers hindering configurational rearrangement in the liquid (see Richet, 1984; Neuville and Richet, 1991; Richet and Bottinga, 1995 for more details).

It is well known that a glass does not undergo significant configurational changes with temperature. The residual entropy of a glass at 0 K is the configurational entropy, which remains constant up to the glass transition temperature, T_g. The configurational changes that take place in a liquid are associated with a configurational heat capacity (Cp^{conf}). For silicates, Cp^{conf} can safely be taken as the difference in heat capacity between the liquid and the glass at T_g (Richet et al., 1986). Hence, one obtains finally for S^{conf}:

$$S^{conf}(T) = S^{conf}(T_g) + \int_{T_g}^{T} Cp^{conf}/TdT. \quad (2)$$

From Eqs. (1) and (2), the viscosity can be fitted as a function of temperature and finally the two parameters A_e, and B_e, and the configurational entropy $S^{conf}(T_g)$ can be obtained.

The configurational entropy can be determined calorimetrically only for melts formed by congruent melting and for which the entropy of fusion can be measured. In contrast, the configurational entropy can be determined by combining Eqs. (1) and (2) for any liquid. The validity of the Adam and Gibbs method was presented in the calculation of the configurational entropy of a pyrope glass which was compared with calorimetric data (Téqui et al., 1991) and using the Adam and Gibbs (AG) equation (Richet, 1984; Neuville and Richet, 1991; Richet and Neuville, 1992; Richet and Bottinga, 1995). These viscosity measurements can be used to determine the configurational entropy in this ternary system using the AG theory.

The configurational entropy theory provides a simple theoretical framework within which both the temperature and composition dependence of the viscosity can be modeled quantitatively. In addition, the entropy data can serve as thermodynamic constraints which are required for phase-equilibrium calculations. Viscosity data for stable liquids near the liquidus temperature are numerous (e.g., Ryan and Blevins, 1987), but accurate viscosity measurements just above the glass transition are still scarce for many melts of industrial or geological interest. This lack of data is especially unfortunate because of the extremely strong variation of viscosity with composition in this temperature range. These viscosity data are also the most significant ones in determining the configurational entropy.

From previous results (Richet, 1984; Neuville and Richet, 1991), the viscosity and the configurational entropy can now be modeled for some simple alkali or earth-alkali silicate systems. However, the effect of replacing an alkali by an earth-alkaline is not well understood.

The configurational entropy gives an idea of the glass structure (Richet, 1984; Richet and Neuville, 1992; Richet et al., 1993; Neuville and Mysen, 1996; Toplis, 1998; Lee, 2005). Neuville and Mysen (1996) have shown that the configurational entropy at the glass transition temperature and Q^n species determined by Raman spectroscopy present similar variations with chemical composition. Q^n denotes a tetrahedral site, SiO_4, where n is the number of bridging oxygen per tetrahedron. Raman spectroscopy is a useful technique to probe the medium range order of glasses and melts. Several Raman spectroscopic studies have been already reported along portions of the binary joins Na_2O–SiO_2 and CaO–SiO_2 (Brawer and White, 1977a,b; Mysen and Frantz, 1992, 1994; Frantz and Mysen, 1995) and some NMR studies on binary and ternary compositions have been published recently (Buckerman and Müller-Warmuth, 1992; Lockyer et al., 1995; Jones et al., 2001). Lee and Stebbins (2003), using NMR for mixed Na–Ca-silicate glasses with high silica content, have proposed that Ca and Na are non-randomly distributed.

The purpose of this paper is the study of the effect of mixing due to Na/Ca substitution on the viscosity, the configurational entropy and the structure of glasses. The configurational entropy presents a non-ideal behavior, which is related to the Q^n variation and the structure of the melts obtained from the Raman spectroscopy.

2. Experimental method

2.1. Starting materials

The samples were obtained by melting mixtures of Na_2CO_3, $CaCO_3$ and SiO_2. About 100 g of $CaCO_3$–Na_2CO_3–SiO_2 (Rectapur from Merck) was ground for 1 h under alcohol in an agate mortar, heated slowly to decompose the carbonates, and then heated above the melting point. The chemical compositions investigated have 60 mol% of SiO_2, which is the SiO_2 limit above which Ca-silicate glasses unmix (Morey and Bowen, 1925; Mysen and Richet, 2005). At lower SiO_2 content, Na-metasilicate crystallizes rapidly from glasses, thus making property measurements unfeasible. The six compositions investigated in this study are reported in Table 1, with the notation CN60.X, where X is the mol% of Na_2O and 60 is the mol% of SiO_2. The mol% of CaO corresponds to $100-(60+X)$. Densities of all glasses measured with Archimedes method using toluene as the immersion liquid, and the liquidus temperature, T_l (from Morey and Bowen, 1925) are also given in Table 1. These glasses were melted in covered Pt crucibles to avoid contamination. The melts were maintained for a few hours at high temperature (1800 K for lime silicate melt and 1300 K for soda rich silicate melt) in air and stirred to obtain the bubble-free products required for the viscosity measurements. The sample was quenched in a few seconds from high temperature by dipping the bottom of the platinum crucible into pure water. The heating procedure was repeated until no crystallization could be detected by optical microscope and X-ray diffractometry. All materials were found to be chemically homogeneous glassy phases before and after viscosity measurements. Glass samples were analyzed with a Cameca SX100 electron microprobe (Table 1 for results and analytical conditions).

The glasses were stored in a desiccator due to the hygroscopic nature of the soda silicate compositions. The water content of the Na-silicate glass (CN60.40) was determined using a vacuum fusion extraction, which indicated the presence of less than 10 ppm water.

2.2. High-viscosity measurements

Viscosity measurements on supercooled liquids were carried out in air, with the creep apparatus described by Neuville and Richet (1991). With this apparatus, a load of up to 500 kg can be applied to the sample. For a 3 mm diameter sample, the maximum stress is 700×10^6 Nm^{-2}, and for a 9 mm diameter sample, the stress is 80×10^6 Nm^{-2}. For these measurements, a temperature gradient can be an important parameter. We therefore used a silver cylinder attached to the upper piston to reduce the temperature gradient along the sample. The temperature was measured with two Pt–Pt/Rh10% thermocouples on top and bottom of the sample; cold junction corrections were made with Omega compensators. The temperature difference along the cylinder was found to be less than 0.2 K. The sample used for the measurement is cylindrical with 5 mm diameter and 10 mm length and an approximate weight of 0.5 g. By comparing with the reported values of relaxed viscosity on SRM 710 glass from the National Bureau of Standards (Napolitano and Hawkins, 1964), we estimate the viscosity uncertainty and the reproducibility to be less than 0.03 log units with this technique (Table 2 and Fig. 1) (see Neuville and Richet, 1991). Within the range of stress applied in the creep experiment (6.6 to 8.9 log Nm^{-2}), the viscosity of the samples is Newtonian (Fig. 2).

2.3. Low-viscosity measurements

The low-viscosity measurements were performed in a vertical tube furnace heated by Super Kanthal 33 elements in air (Neuville, 1992). The crucible was supported in the hot zone of the furnace by an alumina tube. The length of the hot zone was determined by temperature measurement inside the crucible. The

Table 1
Chemical compositions of the soda–lime silicate glasses (in wt.%)[a]

	CN60.00	CN60.05	CN60.10	CN60.20	CN60.30	CN60.40
SiO_2	61.50(13)	61.43(8)	61.10(9)	60.27(11)	59.72(7)	59.14(12)
CaO	38.11(19)	33.49(12)	28.32(14)	18.68(16)	9.39(17)	0.05(5)
Na_2O	0.19(16)	5.37(11)	10.53(7)	20.91(10)	30.99(18)	40.85(11)
d	2.760(2)	2.738(3)	2.700(2)	2.625(1)	2.583(2)	2.519(3)
T_l (K)	1740	1700	1600	1450	1270	1170

[a] Average of 15–20 analyses using a Cameca SX100 on different pieces of glasses for each composition at 15 kV and 10 nA with a 15 s count time; d is the glass room-temperature Archimedean density and T_l, the liquidus temperature from Morey and Bowen (1925). Uncertainties are given in parentheses.

Table 2
Viscosity of the N.B.S. standard glass 710, NS66 and NS80 (in log Poise)

T (K)	NBS710	T (K)	NS66	T (K)	NS80
826.5	13.13	718.6	13.53	717.9	14.75
835.9	12.62	729.1	12.84	727.0	14.29
848.6	12.03	733.9	12.51	740.0	13.58
857.3	11.70	739.3	12.25	757.7	13.00
858.6	11.62	749.2	11.70	764.6	12.45
859.2	11.61	758.2	11.21	776.5	11.90
859.7	11.59	774.1	10.58	788.8	11.54
867.5	11.31	786.0	10.11	800.4	11.12
869.3	11.20	795.2	9.85	809.9	10.83
869.6	11.17	797.8	9.73	824.2	10.29
881.4	10.74	805.5	9.51	828.1	10.20
892.0	10.39	1041.0	5.16[c]	836.0	9.98
903.7	10.00	1052.0	3.92	1432.3	3.03
912.1	9.72	1209.1	3.52	1478.2	2.80
1069.2	6.34	1261.1	3.22	1521.6	2.65
1134.2	5.50	1317.1	2.89	1584.2	2.44
1200.6	4.76	1364.6	2.67	1623.4	2.31
1258.8	4.22	1414.6	2.45	1664.7	2.17
1315.2	3.79	1462.4	2.26	1712.4	2.05
1369.7	3.43	1516.7	2.05	1759.3	1.91
1423.2	3.13	1564.6	1.88		
1469.5	2.89	1597.1	1.80		
1513.7	2.69	1661.8	1.61		
1569.1	2.47	1706.8	1.43		
1604.2	2.33	1805.1	1.18		
1675.2	2.08				
1710.6	1.97				
1775.7	1.79				

c=Crystallization of the liquid.
TVF equations for these liquids: NBS710 log η=1.64+4251.6/(T−538.3) AAD 0.04.
NS66 log η=−1.38+3540/(T−479) AAD 0.04.
NS80 log η=−6.4+87500/(T−301) AAD 0.04.
AG equations for these liquids.
NS66 log η=−0.85+79630/(T∗(8.02+14.14∗ln(T−726)) AAD 0.04 where T_g=726K.
NS80 log η=−0.89+1016000/(T∗(9.67+14.02∗ln(T−751)) AAD 0.04 where T_g=751K.
AAD=average absolute deviation.

vertical and radial temperature gradients inside the crucible are respectively less than 2 K for 5 cm (vertical gradient) and 1 K for 2.7 cm (radial gradient) at 1500 K and a little less at 1800 K. The viscosity was measured between 1150 K and 1950 K, with the concentric cylinder method developed by Couette (1888, 1890). The melts were contained in a cylindrical PtRh15% or PtIr10% crucible (50 mm height, 27 mm inner diameter, 1 mm wall thickness). The rotating cylinder size was 14 mm in diameter, 21 mm in height and had 23° conical extremities to reduce termination effects and a 5 mm diameter stem. The viscosity was measured with a Rheomat 115 viscometer head from Mettler, where the cylinder rotates at constant angular velocity between

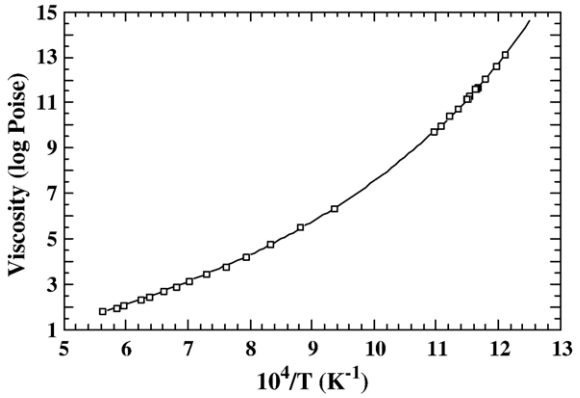

Fig. 1. Viscosity of NBS710 melts measured with the creep apparatus for the high-viscosity range and with the concentric cylinder viscometer for the low-viscosity data. The curve shows the standard NBS values (U.S. National Bureau of Standards).

0.05515 and 780 rpm. The torque exerted on the cylinder by the sample was recorded digitally. This rotating viscometer design was calibrated with the NBS sample SRM 710a for which the viscosity–temperature relationship is accurately known. The precision of viscosity measurements was tested with NBS standard SRM 710 (Napolitano and Hawkins, 1964), which shows that the uncertainty and the reproducibility are within 0.04 log Poise with this technique (Table 2 and Figs. 1 and 2).

2.4. Low- and high-viscosity measurements

The link between high- and low-viscosity measurements is very important. To demonstrate that our two apparatus produce accurate results, we present new measurements on two sodium silicate melts with 66%

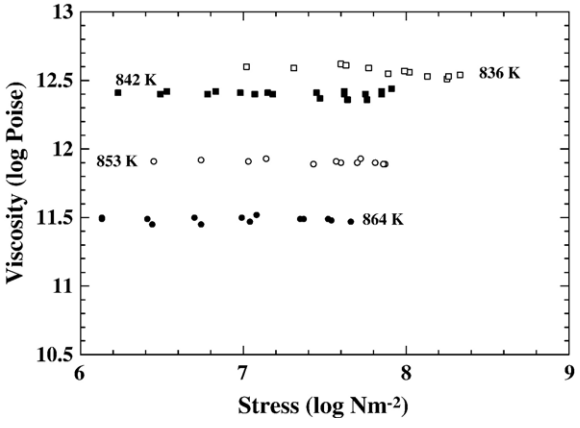

Fig. 2. Viscosity versus applied stress for NBS710 glass during high-viscosity measurements at different temperatures.

(NS2=NS66.00) and 80% (NS4=NS80.00) of SiO_2 for which the viscosities are already well known. The results of the viscosity measurements on these supercooled liquids are listed in Table 2 and are plotted in Fig. 3. For each temperature, using several stresses, the reported viscosities (average of more than 35 measurements) obtained at different stresses show standard deviations less than 0.02 log units. For the NS66.00 and NS80.00 compositions, our data are in very good agreement with those of Shartsis et al. (1952), Fontana and Plummer (1979), Meiling and Uhlmann (1977), Poole (1948), and Bockris et al. (1955). The gap between high- and low-viscosity measurements corresponds to the temperature intervals where measurements are not possible because of the rapid crystallization of the melt. The crystallization effect on viscosity is illustrated by the NS66 curve in Fig. 3 for a viscosity close to 5.16 log Poise where we observed an increase of viscosity as a function of time at constant temperature. This behavior was already described by Lejeune and Richet (1995).

2.5. Raman spectroscopy

The measurements were made with a T64000 Jobin-Yvon confocal microRaman spectrometer equipped with a CCD detector. The 514.532 nm line of a Coherent 70-C5 Ar^+ laser operating at 2.8 W at the sample was used for sample excitation. For the samples examined here, this excitation and CCD system result in a signal-to-noise ratio of 80/1. The integration time was 60 s. With our triple spectrometer, it is possible to take spectra at a very low frequency (less than 10 cm^{-1}). All reported spectra are unpolarized. To study the structure of glasses, where the Si–O vibrations are located at about 1000 cm^{-1}, the spectra were corrected for the temperature- and frequency-dependent scattering intensity before statistical analysis (Mysen, 1990). A correction factor of the form proposed by Long (1977) and given correctly by Neuville and Mysen (1996) was used. The corrected Raman intensities were normalized to the data point of the greatest absolute intensity. The spectra were deconvoluted with the method of minimization of least squares described by Davidon (1966) (see also Seifert et al., 1982; Mysen et al., 1982; Mysen, 1990; Mysen and Frantz, 1994 for a detailed discussion). During curve-fitting, all band parameters (frequency, half-width and intensity) are independent and unconstrained variables. The number of lines fitted to a spectrum was treated statistically by minimization of the residual, χ^2 and by maximizing the randomness of the residuals according to Mysen (1990). For all compositions except for the high soda content glass, χ^2 decreases from 5000, 100 and 5.3 when we use 2, 4 and 5 bands, respectively. For the high soda content glass, the χ^2 is similar for 4 bands ($\chi^2=2.8$) and for 5 bands ($\chi^2=2.7$). To check the variation in the low-frequency region (boson area), the spectra were not normalized, and are reported in counts per second.

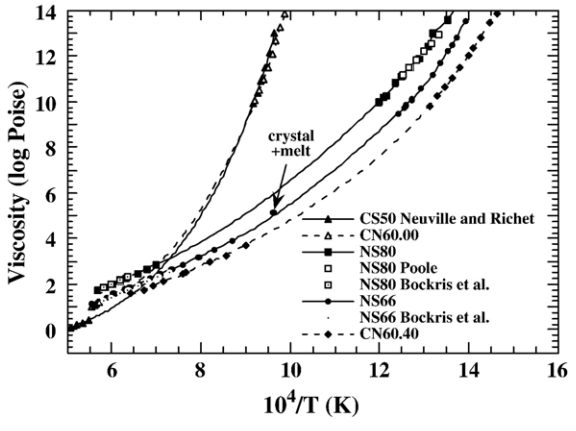

Fig. 3. Viscosity of the simple soda or lime silicate melts, and comparison with previous work by Neuville and Richet (1991) on a calcium metasilicate glass (CS50), by Poole (1948) on soda tetrasilicate melts (NS80) and by Bockris and co-workers (1955) on soda disilicate (NS66) and tetrasilicate melts (NS80).

3. Results

3.1. Viscosity measurements

The results of viscosity measurements on supercooled liquids are listed in Table 3 for each temperature, averaged over 20 or 30 measurements made at different stresses. In Fig. 4, the viscosity data for the soda–lime silicate glasses and melts were plotted as a function of reciprocal temperature. The Ca-silicate liquids (CN60.00 and CN60.20) crystallized rapidly in the sub-liquidus region, and we observed an increase of the viscosity with time at constant temperature. Such measurements do not correspond to a pure silicate liquid but rather to a mixture of crystals and liquid. Therefore, the values marked with c in Table 3 are not plotted in Fig. 4. In this system, no viscosity measurements between 10^3 and 10^{10} Poise are possible because of the very rapid rate of crystallization in this viscosity–temperature range (Meiling and Uhlmann, 1977; Mastelaro et al., 2000).

In Fig. 4, we observe that the addition of 10 mol% Na_2O to a lime silicate melt modified the viscosity more than the addition of 10 mol% CaO to a soda silicate melt. A striking difference exists in the behavior of the

Table 3
Viscosity for melts (in log Poise)

CN60.00		CN60.05		CN60.10		CN60.20		CN60.30		CN60.40	
T (K)	log η	T (K)	log η	T (K)	log η	T (K)	log η	T(K)	log η	T(K)	log η
1012.2	13.87	942.1	13.30	892.5	13.41	803.1	13.93	737.1	13.78	684.0	13.90
1022.9	13.31	952.7	12.69	899.8	13.03	812.2	13.44	747.3	13.13	691.2	13.53
1033.2	12.71	963.3	12.12	906.4	12.65	821.1	12.91	756.1	12.65	701.6	12.92
1043.7	12.09	973.5	11.67	912.9	12.26	828.2	12.46	762.1	12.24	709.8	12.36
1053.4	11.53	983.2	11.17	918.8	11.98	832.6	12.17	766.1	12.03	715.1	12.02
1063.9	10.99	994.4	10.68	927.8	11.50	838.2	11.92	772.9	11.65	724.9	11.51
1075.3	10.50	1004.5	10.29	933.6	11.22	848.0	11.38	780.8	11.22	734.2	11.06
1085.8	10.06	1014.4	9.92	943.4	10.78	853.0	11.15	783.6	11.13	742.9	10.64
1722.1	2.43[c]			954.6	10.34	862.3	10.70	795.7	10.52	752.2	10.25
1723.0	2.38[c]			965.1	9.97	869.4	10.40	807.6	10.02	762.9	9.81
1738.0	1.95[c]					876.3	10.13	817.2	9.69	1113.2	3.72
1738.8	1.36[c]					886.8	9.69			1170.0	3.27
1739.8	1.52[c]					1370.6	4.84[c]			1222.4	3.00
1743.8	1.43[c]					1412.1	2.72[c]			1304.3	2.55
1749.6	1.23					1414.4	3.28[c]			1317.7	2.49
1751.1	1.35[c]					1432.8	2.20			1319.1	2.45
1753.7	1.36[c]					1445.5	2.15			1400.8	2.14
1760.2	1.21					1449.5	2.10			1444.3	1.97
1760.0	1.21					1457.6	2.06			1492.1	1.78
1771.9	1.17					1475.4	2.01			1563.2	1.54
1785.8	1.12					1480.8	1.97				
1809.5	1.06					1496.1	1.89				
						1562.9	1.66				

Crystallization of the liquid, these data were not used to calculate the TVF and AG coefficients given in Table 5.

viscosity between pure Na-silicate liquid (CN60.40) and pure Ca-silicate liquid (CN60.00) (see Fig. 5). Indeed, at constant viscosity, close to the glass transition (13 log Poise) (Fig. 4), the difference in temperature is greater than 300 K between pure soda and lime silicate glasses. This difference decreases with increasing temperature and becomes lower than 100 K at 1600 K. Moreover, at the same temperature near 1000 K, we observed as a function of $Na_2O/(Na_2O+CaO)$ a difference in viscosity of 10 orders of magnitude between pure soda and pure lime silicate compounds (Fig. 5), while this difference is less than 1 order of magnitude at high temperature (1600 K).

At high temperature (1600 K), the viscosity of silicate melts varies linearly with $Na_2O/(Na_2O+CaO)$, with a small decrease as the content of Na_2O increases (Fig. 5). For temperatures near the glass transition temperature, the viscosity deviates negatively from a linear variation.

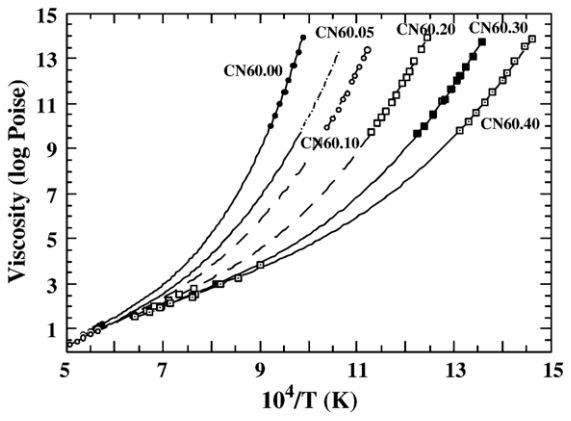

Fig. 4. Viscosity versus reciprocal temperature for silicate melts ranging from the pure lime silicate melt (CN60.00) to pure soda silicate (CN60.40). Curves are calculated with the Adam and Gibbs equation, with the parameters given in Table 4.

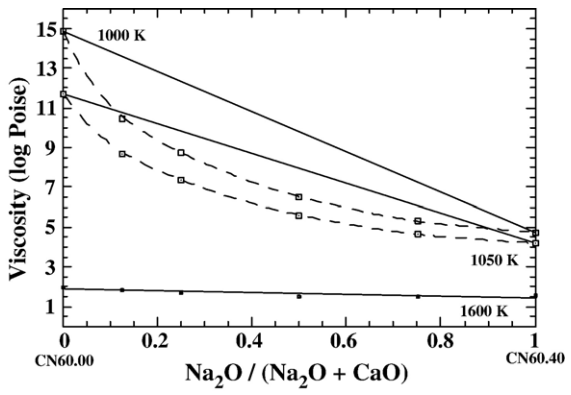

Fig. 5. Viscosities of soda–lime silicate melts versus $Na_2O/(Na_2O+CaO)$ at constant temperature.

The deviation from a linear variation is 4 orders of magnitude at 1000 K and only 2.5 orders at 1050 K and increases with decreasing temperature. Similar behaviors were already observed first by English (1923) in the same system with 75 mol% of SiO_2, 25 mol% of Na_2O, and with a substitution up to 12 mol% of CaO, second in the compilation made by Bansal and Doremus (1986) for melts with 65 and 70 mol% of SiO_2. But in all these cases, the viscosity measurements cannot be made for the lime silicate compositions.

Near the glass transition (viscosities between 10^{10} and 10^{14} Poises), the relationship between log η and $1/T$ is not linear (Fig. 4) which indicates that the viscosity of these melts does not follow an Arrhenian behavior. These high-viscosity measurements can be fitted using a Tamman–Vogel–Flucher (TVF) equation:

$$\log \eta = A + B/(T - T_1), \quad (3)$$

where A, B, and T_1 are adjustable parameters given in Table 4. This equation was used only to fit the low-temperature viscosity measurements since the extrapolation to higher temperature is not feasible. Indeed, with this equation, it is not possible to extrapolate the low-temperature viscosity data to higher temperature (Neuville and Richet, 1990). In order to model the whole temperature range (high and low) and to link viscosity to configurational entropy, we need to use the Adam and Gibbs equation (Eq. (1)) (Neuville and Richet, 1990).

3.2. Raman spectroscopy

Adding CaO to the Na-silicate glasses modifies the Raman spectra (Fig. 6). In this paper, we focus only on the Raman spectra of glasses at room temperature, which provide the most important configurational information on the structures. In fact, from the Raman spectra at high temperature, we can obtain some structural information on the liquid, but this information cannot be compared with the configurational entropy obtained from the viscosity measurements (Neuville and Mysen, 1996). Variation of Q species at room temperature obtained by Raman spectroscopy can show behavior similar to that observed for the configurational entropy (Neuville and Mysen, 1996).

The Raman spectra were recorded between 10 and 1300 cm^{-1}. The spectra can be divided into four regions: the boson region (10–250 cm^{-1}); the low frequency region (250–700 cm^{-1}); the medium frequency region (700–850 cm^{-1}); and the high frequency region (850–1300 cm^{-1}). The boson region was studied without normalization. The most important structural information is gained from the Si–O stretch frequencies with the Raman bands in the 850–1200 cm^{-1} region (see for example; Seifert et al., 1982; Mysen, 1988). For the soda silicate glass (CN60.40), we observe in Fig. 6 five peaks at 580, 596, 768, 950 and 1079 cm^{-1} (extracted from differentiation of the spectra using Igor@ software), which agrees with Brawer (1975) and Brawer and White (1977a,b). These peaks evolve in intensities and in frequency as a function of CaO content in such a way that the spectrum for the lime silicate glass (CN60.00) presents a large peak at 608 cm^{-1} and other peaks at 790, 965 and 1044 cm^{-1}. These results are consistent with those already observed for soda silicate by Brawer and White (1977a,b), and for lime silicate by Frantz and Mysen (1995).

Table 4
TVF, AG parameters: data in K, J/mol, J/mol K

	CN60.00	CN60.05	CN60.10	CN60.20	CN60.30	CN60.40
A	−2.99	−2.86	−2.50	−2.13	−1.53	−1.47
B [a]	4.18	4.40	4.11	3.72	3.32	3.36
T_1	765.6	669.9	634.8	572.8	521.1	466.1
$T\eta$	1027.1	947.3	899.9	818.8	749.5	698.5
AAD [b]	0.04	0.01	0.02	0.03	0.02	0.03
$Cp_g(T\eta)$ [c]	65.8	66.5	67.7	69.9	72.1	74.5
Cp_l [c]	83.2	84.0	84.7	86.2	87.6	89.1
Cp^{conf}	17.5	17.4	17.0	16.3	15.5	14.6
A_e	−2.02	−1.87	−1.56	−1.16	−0.72	−0.55
B_e [a]	85.47	94.29	86.48	74.35	65.47	63.57
S^{conf} (T_g)	5.53	6.69	6.61	6.41	6.36	6.72
AAD	0.03	0.02	0.03	0.03	0.03	0.03
T_0	749.	645.	610.	552.	497.	441.

[a] B and B_e are divided by 1000.
[b] Average absolute deviation.
[c] Values calculate using the Richet (1987) and Richet and Bottinga (1985) models.

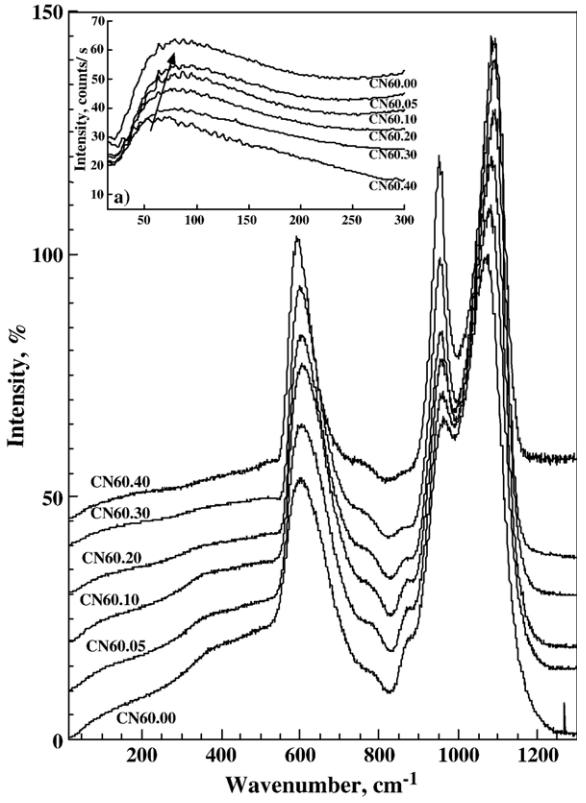

Fig. 6. Raman spectra at room temperature for soda–lime silicate glasses. Insert: region at low frequencies corresponding to the Boson peak.

3.2.1. The boson region (10–250 cm^{-1})

Below 250 cm^{-1}, there is only a scattering continuum and the Raleigh tail of the exciting line, except at very low frequency where there is the so-called boson peak (Malinovsky and Sokolov, 1986; Buchenau et al., 1986). This peak has been ascribed to excitations associated with rotational motions of almost rigid tetrahedra (Buchenau et al., 1986; Hehlen et al., 2000, 2002). Hehlen et al. (2002) consider that this peak, observed for different silicate glasses, increases in intensity and shifts to higher frequency with higher distortion of the SiO_4 tetrahedra. In our case, an increase in intensity and a shift to high frequency were observed when CaO replaced Na_2O. In the Table 5, the frequencies of the boson peaks are given. The frequency of the boson peak varies linearly with composition (frequency = 82.542 − 0.448xNa_2O).

3.2.2. The low frequency region (250–700 cm^{-1})

The Raman spectrum above 500 cm^{-1} is due primarily to the vibrations of the Si–O network with the modifiers essentially at rest (Phillips, 1984). A weak band at 390 cm^{-1} observed for the lime silicate glass disappears when more than 10 mol% of Na_2O is added. In the CN60.40 glass, the peaks at 580 and the shoulder at 600 cm^{-1} evolve into only one broad peak, which becomes less asymmetric with the addition of CaO content. The peak at 580 cm^{-1} is assigned to Si–O^0 rocking motions in fully polymerized SiO_2 (Q^4) units (Bell and Dean, 1972; Phillips, 1984). The maximum at 600 cm^{-1} is assigned to Si–O–Si bending motions in depolymerized structural units (Lazarev, 1972; Furukawa et al., 1981).

3.2.3. The intermediate frequency region (700–850 cm^{-1})

The broad peak at 755 cm^{-1} for the CN60.40 glass shifts to higher frequency with increasing CaO content (790 cm^{-1} for CN60.00). This observation is in good agreement with Frantz and Mysen (1995) who observed that this peak shifts to higher frequencies with increasing the size of the cation, in the order Ca < Sr < Ba.

3.2.4. The high frequency region (850–1300 cm^{-1})

The 950 and 1085 cm^{-1} peaks in the Raman spectra of CN60.40 evolve to one broad peak at 1050 cm^{-1} and a smaller peak at 965 cm^{-1} with increasing CaO content. From the differentiation of the spectra, we observe that the position of the peak at 950 cm^{-1} shifts to higher frequencies when adding CaO (965 cm^{-1}). A similar increase in frequency is observed for the peaks at 755 and 580 cm^{-1} upon addition of CaO content whereas the peak at 1050 cm^{-1} decreases in frequency with higher CaO content (Table 5). These findings for the soda and lime silicate glasses are in good agreement with those reported by Brawer and White (1977a,b) and Mysen and Frantz (1992, 1994) on NS2 glass (sodium disilicate composition, 33 mol%Na_2O, 66 mol% SiO_2) and by Frantz and Mysen (1995) on CS1.5 glass (40 mol %CaO, 60 mol% SiO_2).

3.2.5. Spectra deconvolution

It is well known (Mysen, 1988) that peak areas do not represent totally the Q species concentrations, but in these systems, we can consider that the relative cross sections do not change with composition as a first approximation. The high-frequency region (850–1300 cm^{-1}) of the Raman spectra of the six glasses has been deconvoluted with a technique previously described (Mysen et al., 1982; Mysen, 1990) using four or five Gaussian bands at 870, 950, 1000, 1050 and 1150 cm^{-1}. The frequency, width and area of each Gaussian band are given in Table 5. In Fig. 7, typical fits were reported for CN60.00, CN60.20 and CN60.40 glasses. The assignments of the 870, 950, 1100 and

Table 5
Frequencies of peak positions obtained by differentiation of Raman spectra and Raman bands obtained from the deconvolution fits (data in cm^{-1})

	CN60.00	CN60.05	CN60.10	CN60.20	CN60.30	CN60.40
Frequencies of peaks						
Boson	82	80	78	73	69	62
ν_{600}	608	606	605	602	597	596
ν_{800}	790	788	784	780	772	768
ν_{950}	965	961	959	952	950	950
ν_{1050}	1044	1048	1054	1069	1074	1079
Bands deconvolution						
V1	871.0	872.0	872.1	885.2		913.1
V2	961.1	956.3	957.1	953.0	952.9	950.0
V3	1020.0	1030.3	1024.2	1035.2	1054.1	1039.9
V4	1072.1	1084.1	1084.2	1093.0	1096.4	1091.8
V5	1135.0	1129.0				
W1	41.1	44.2	36.3	62.3		37.0
W2	85.2	74.7	71.7	58.3	54.1	40.3
W3	53.1	68.2	57.6	75.8	94.0	110.0
W4	77.1	67.5	76.8	64.6	52.3	58.6
W5	89.8	90.6				
A1	394.0	375.8	214.0	246.1		248.1
A2	5244.0	4079.2	3895.4	2943.0	2973.0	2416.1
A3	1452.1	3491.1	2208.3	3613.1	5339.2	3750.1
A4	7385.0	5625.1	7698.2	5958.1	3678.1	4322.1
A5	995.0	1161.1				

V2, W2, A2 correspond of the frequency, the width and the area for the Q^2 species, and the V4, W4, A4 for the Q^3 species and V5, W5, A5 for the Q^4 species.

1150 cm^{-1} bands correspond to Si–O stretch vibrations in specific structural units (Furukawa et al., 1981; McMillan, 1984; Mysen and Frantz, 1994; Frantz and Mysen, 1995). The small band at 870 cm^{-1} can be attributed to the $Si–O^-$ stretching in tetrahedra with three non-bridging oxygen per silicon (NBO/Si=3; Q^1). The band near 950 cm^{-1} is assigned to $Si–O^-$ stretching in structural units with two non-bridging oxygen per silicon (NBO/Si=2; Q^2). The main band centered near 1050 cm^{-1} is due to the $Si–O^-$ stretching in units with one non-bridging oxygen per silicon (NBO/Si=1; Q^3). The high-frequency band at 1150 cm^{-1} results from the presence of fully polymerized units (Q^4). The large band at slightly lower frequency, 1000 cm^{-1}, has been interpreted as a vibrational frequency assignable to a $Si–O^0$ bridging oxygen stretching mode (Mysen and Frantz, 1994) or alternatively as a vibration in structural units associated with the metal cation (Fukumi et al., 1990).

The position of the bands assigned to Si–O stretching in Q^4 and Q^2 units decreases in frequency with increasing the Na_2O content whereas the positions of the three others bands, Q^3, Q^1 and 1000 cm^{-1} shift to higher frequency with increasing Na_2O content (Fig. 8). The shift in frequency of the 1000 cm^{-1} band is in good agreement with the idea developed by Fukumi et al. (1990) who attributed it to a vibration in structural units associated with the metal cation. Indeed, the NBO–Na bonding is weaker than the NBO–Ca bonding even if the frequency of this bonding can be higher than those of the Q-Ca vibrations.

The Q^1 and Q^4 species occur in very small amounts (Table 5). This agrees with previous NMR results (Buckerman and Müller-Warmuth, 1992; Jones et al., 2001) and Raman spectra (Mysen and Frantz, 1992, 1994; Frantz and Mysen, 1995) that indicate the presence of the Q^4, Q^3, and Q^2 species in rich-SiO_2 silicate glasses, like sodium disilicate NS2, and the presence of Q^1 species only in the poor-SiO_2 glasses, like CS1.5 (Frantz and Mysen, 1995; Buckerman and Müller-Warmuth, 1992; Brawer and White, 1977a,b).

4. Discussion

4.1. Adam and Gibbs theory and configurational entropies

As already observed for natural magmas compositions (Neuville et al., 1993) and industrial glasses (Sipp et al., 1997), Eqs. (1) and (2), proposed by Richet (1984), are valid for complex compositions as well as for simple melts (Neuville and Richet, 1991). Configurational entropy obtained from viscosity or from calorimetry measurements is equal (Téqui et al., 1991; Neuville and

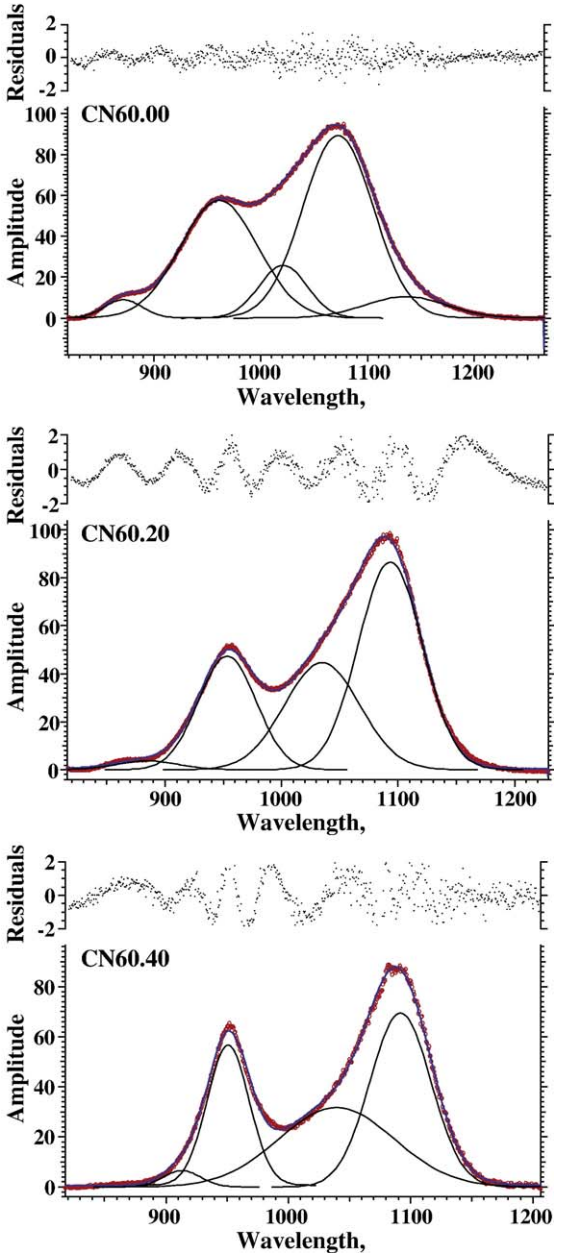

Fig. 7. Curve fitted Raman spectra of the soda–lime silicate glasses.

Richet, 1991; Richet et al., 1993; Richet and Bottinga, 1995). Therefore, it is not surprising that we obtained a quantitative validity of the equations for the melts investigated in this study. As previously shown (Neuville and Richet, 1990), it is necessary to use the Adam and Gibbs equation of viscosity to extrapolate the viscosity measurements. The Arrhenius or TVF equation can only be used to interpolate viscosity measurements.

The configurational heat capacity, Cp^{conf}, is required in order to determine the configurational entropy, $S^{conf}(T)$, from Eqs. (1) and (2). This configurational heat capacity is taken following Richet et al. (1986) using the difference between the heat capacity of the liquid and that of the glass at the glass transition temperature (T_g). Configurational heat capacity can be measured (see Richet, 1987; Richet and Bottinga, 1985) or determined by calculation. This calculation was performed by using the model proposed by Richet (1987) for the heat capacity of glasses and by Richet and Bottinga (1985) for the heat capacity of the liquid. From these models, constant values were obtained for the heat capacity of the glass at the glass transition temperature $Cp_g(T_g)$, and also for the heat capacity of the liquid Cpl which for soda and lime silicate liquid is temperature-independent (Richet and Bottinga, 1985). We have already shown that these models work very well for natural glasses (Neuville et al., 1993) and industrial glasses (Sipp et al., 1997; Richet et al., 1997). From these models, we observed an increase of the configurational heat capacity with the increase of lime in the silicate melts. This increase results essentially from the strong difference between the partial molar heat capacity of CaO compared to Na_2O (see Richet, 1987).

Using this configurational heat capacity, and Eqs. (1) and (2), the viscosity measurements at high and low temperature can be fitted, and the configurational entropy can be determined for each chemical composition between lime (CN60.00) and soda (CN60.40) silicate glasses (Table 4). The configurational entropy at T_g, $S^{conf}(T_g)$, and the other parameters of the Adam and Gibbs equation are given in Table 4 and plotted in Fig. 9 as a function of Na_2O content. A_e and B_e are independent of temperature for a given composition but vary as a function of the composition of the melt (Table 4) (Toplis, 1998 for more details). The error bars of 5% for

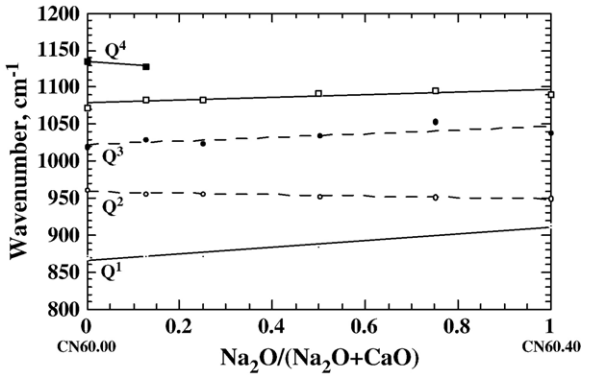

Fig. 8. $Na_2O/(Na_2O+CaO)$ dependence of Raman frequencies of the 1190 (Q^4), 1060 (Q^3 species), 1010, 950 (Q^2) and 870 cm^{-1} (Q^1) bands obtained from the fits.

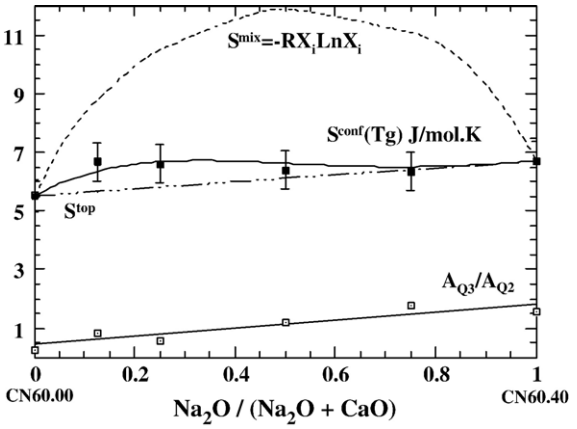

Fig. 9. $Na_2O/(Na_2O+CaO)$ dependence of configurational entropy, $S^{conf}(T_g)$, A_{Q3}/A_{Q2} ratio (entropies are in J/mol K and A_{Q3}/A_{Q2} is dimensionless).

the configurational entropy parameters were described and discussed by Neuville and Richet (1991).

Between lime and soda silicate glasses, the $S^{conf}(T_g)$ shows a non-linear variation. The configurational entropy increases by nearly 30% with the addition of less than 5 mol% of Na_2O to the lime silicate glass, CN60.00. With increasing Na_2O content, the configurational entropy remains nearly constant around 6.5 J/mol K (CN60.05) up to 6.9 J/mol K for the pure soda silicate glass (CN60.40). For alkali (Richet, 1984) and alkaline-earth elements (Neuville and Richet, 1991), the configurational entropy can be calculated using an ideal mixing term such as $-RnX_iLnX_i$ with $X_i=Ca/(Ca+Mg)$ or $Na/(Na+K)$, R is the gas constant and n the number of atom exchange (see also Richet, 2001). This ideal mixing term can be interpreted as a random distribution for Ca and Mg or for K and Na in the silicate or aluminosilicate network (Richet, 1984; Neuville and Richet, 1991). In the present case, a good fit of the configurational entropy cannot be obtained using this ideal mixing term (see Fig. 9, dotted line). Instead, the fits of the configurational entropy presented in Fig. 9 require a non-ideal mixing term to be added into the configurational entropy equation:

$$S^{conf}(T_g) = S^{mix} + \sum x_i S_i^{conf}(T_g), \quad (4)$$

where S_i^{conf} is the topological entropy of the end-members i that can be represented by the linear variation (linear dash-dotted line in Fig. 9), and S^{mix} is a non-ideal mixing entropy between Na and Ca in this system. This term can be expressed using:

$$S^{mix} = W_{NC} x_n y_c^3, \quad (5)$$

where $x_n=Na_2O/(Na_2O+CaO)$ and $y_c=1-x_n$, and W_{NC} is a constant equal to 8.14. In the present soda–lime silicate system, two sodium atoms replace one calcium atom. This substitution implies a significant change in the residual entropy and in the glass structure. This term corresponds to a mixing effect between Na_2O–CaO and is not temperature-dependent. This small increase in the configurational entropy for mixed Na/Ca-silicate glasses is in good agreement with the finding of Lee and Stebbins (2003) based upon ^{23}Na and ^{17}O NMR spectroscopy.

Using Eqs. (4) and (5), we can reproduce satisfactorily the entropy variations in Fig. 9.

With these results, we first calculate the temperature T_o at which the configurational entropy would be equal to 0 (Table 4). This temperature would be the same as that of the Kauzmann paradox (Kauzmann, 1948), which is at the basis of the Adam and Gibbs theory, considering that the vibrational entropy of the glass and crystal phases is the same. Similar to a previous study (Sipp et al., 1997), the T_o temperatures agree well with the empirical temperatures T_1 derived from the TVF Eq. (3) for all glasses (Table 4). Given the rather wide range of temperature used in the calculations and the extrapolations of the Cp^{conf} data, this result is a good proof of the consistency of our study. For the glasses here investigated, T_1 and T_o present a rapid decrease with addition of Na_2O.

4.2. Network polymerization

When adding up to 30 mol% of Na_2O to the lime silicate glass, we observed that the configurational entropy increases (Fig. 9). This finding suggests an increase of the disorder in the glass and/or a change in the glass network polymerization. Structural changes that may account for the entropy evolution may be discerned in the Raman spectra of the glasses (Neuville and Mysen, 1996). From Raman spectroscopy, the network polymerization is evaluated in terms of Q^n species. In Fig. 9, the ratio A_{Q3}/A_{Q2} is plotted as a function of $Na_2O/(Na_2O+CaO)$ and corresponds to the ratio of the area of the bands used in the deconvolution of the Raman spectra given in Fig. 7. This ratio represents a variation of the Q^n species that indicates a change in the Q^n speciation distribution. There is a distinct increase of this ratio with adding Na_2O in the lime silicate glass.

This modification of the Q^n speciation is consistent with NMR studies (Maekawa et al., 1991; Buckerman and Müller-Warmuth, 1992; Jones et al., 2001) that have shown an increase of Q^3 with adding Na_2O in a Ca–Na-silicate glasses.

The increase of Q^2 species with increasing CaO content in the soda silicate glasses can be correlated to

the observation of the increase in the frequency position and in the intensity of the boson peak. These changes in the boson peak may correspond to an increase of the distortion of the tetrahedra (Hehlen et al., 2002), suggesting that Q^2 units are more distorted than Q^3 or Q^4 units. This assumption can also be confirmed by molecular dynamics (Vedishcheva et al., 1995; Zotov and Keppler, 1998; Cormack and Du, 2001) where they show that Si–BO average distances are shorter than Si–NBO average distance (BO is a bridging oxygen and NBO a non-bridging oxygen). This implies that Q^4, with 4 BO, are more regular tetrahedra than Q^3 or Q^2 with two mean average distributions for the Si–BO and Si–NBO.

4.3. Fragility

Angell (1991) proposed a classification of liquids between strong and fragile. A strong liquid shows a linear variation in a log η versus T_g/T diagram, while this linear relation is not preserved in a fragile liquid. The configurational entropy also affects the fragility of silicate melts. The viscosities of the soda–lime silicate melts are plotted as a function of T_g/T in Fig. 10. The strongest liquid is the pure soda silicate (CN60.40) while the most fragile liquid is the pure lime silicate (CN60.00). Other intermediate chemical compositions present intermediate behavior between CN60.40 and CN60.00. In Table 4, we give the configurational heat capacity using the models developed by Richet (1987) and Richet and Bottinga (1985). From these values of heat capacities, we calculate the Cp^{conf} value, which shows a decrease of about 20% when replacing Ca by Na. These results for the heat capacity are in good agreement with those observed from the fragility determined by the viscosity.

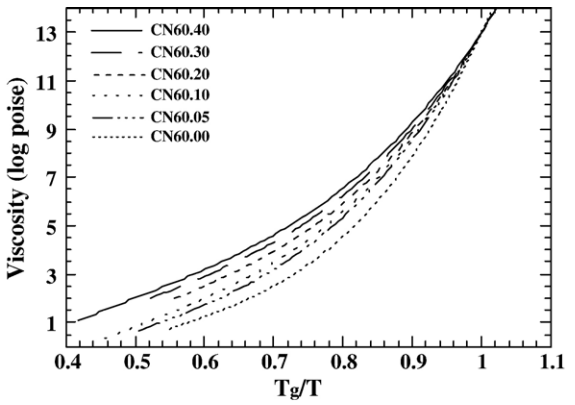

Fig. 10. Viscosity of soda–lime silicate glasses versus T/T_g.

4.4. Configurational entropy, fragility, Q^n species, mobility and connectivity of the network

The cation distribution in the glass network can have important implications for the transport properties such as viscosity and conduction. The observation in mixed Na–Ca glasses (Roling and Ingram, 2000) that the mobility of the Ca^{2+} cation is enhanced when replaced by Na^+ which thus has a positive coupling effect on the movements of divalent cations, is well correlated with the increase in S^{conf} when adding Na_2O in Ca-silicate glass. Conversely, the activation energies related to the movement of Na^+ are slightly changed. The cation mobility is strongly dependent on the glass structure. Therefore, the structural changes taking place during the Ca/Na substitution facilitate the displacement of Ca^{2+}. The modification in network topology will provide new types of empty sites that could be used for Ca movements (Cormier and Neuville, 2004). The mobility of the divalent cation is then assisted by positive coupling with the more mobile monovalent cation (Magnien et al., 2004).

The configurational entropy variation does not follow an ideal mixing term, which implies that the Na and Ca atoms are not randomly distributed in the silicate network, contrary to Na–K or Ca–Mg in silicate liquids (Richet, 1984; Neuville and Richet, 1991). This observation is also in good agreement with the results determined by ^{17}O and ^{23}Na NMR spectroscopy (Lee and Stebbins, 2003), showing that the Na–Ca distributions deviate from a random distribution. From Raman spectroscopy, it is difficult to determine a non-random distribution. More information concerning the silicate network can be gained. We observe that the proportion of Q^2 species increases relatively with CaO content and in the same way, the intensity and the frequency position of the boson peak increases. From this observation, we can make the assumption that the distortion of the tetrahedra and the distortion of the network increase with increasing CaO content (Cormack and Du, 2001). This conclusion is also well correlated with the fragility that increases with CaO content. These conclusions are in good agreement with those observed on Na/Sr substitution in silicate melts (Neuville, 2005).

5. Conclusions

In this paper, we present some new viscosity measurements and Raman spectra on glasses in the SiO_2–Na_2O–CaO system. We can conclude that:

– The viscosity decreases rapidly with increasing Na_2O content in the Ca-silicates.

- The configurational entropy shows non-ideal mixing entropy when replacing Na_2O by CaO which implies a non-random distribution of Na and Ca in the silicate network.
- The fragility of the liquid decreases with adding Na_2O in the Ca-silicate melts.
- The AQ^3/AQ^2 ratio increase with adding Na_2O in the Na-silicate melts.

Acknowledgments

Thanks to S. Vignesoult from Saint-Gobain Recherche for providing the NBS710; M. Wolf from the Library of the Carnegie Institution of Washington for supplying old reprints of G.W. Morey's works. Ongoing discussions with Dominique de Ligny, Laurent Cormier, Bjorn Mysen, Jonathan Stebbins, Pascal Richet are very appreciated. IPGP contribution 2115. **[RR] [JS]**

References

Adam, G., Gibbs, J.H., 1965. On the temperature dependence of cooperative relaxation properties in glass-forming liquids. J. Chem. Phys. 43, 139–146.

Angell, C.A., 1991. Relaxation in liquids, polymers and plastic crystals strong/fragile patterns and problems. J. Non-Cryst. Solids 131–133, 13–31.

Bansal, N.P., Doremus, R.H, 1986. Handbook of Glass Properties. Academic Press. 680 pp.

Bell, R.J., Dean, P., 1972. Localization of phonons in vitreous silica and related glasses, In: Douglas, R.W., Ellis, B. (Eds.), International Conference on the Physics of Non-Crystalline Solids, 3rd. Wiley-Interscience, pp. 443–452.

Bockris, J.O.M., Mackenzie, J.D., Kitchener, E., 1955. Viscous flow in silica and binary liquid silicates. Faraday Soc. Lond. Trans. 51, 1734–1749.

Boow, J., Tech, B.S., Turner, W.E.S., 1942. The viscosity and working characteristics of glasses: Part 1. The viscosity of some commercial glasses at temperature between approximately 500° and 1400°. J. Soc. Glass Technol. 26, 215–240.

Brawer, S.A., 1975. Theory of the vibrational spectra of some network and molecular glasses. Phys. Rev., B 11, 3173–3194.

Brawer, S.A., White, W.B., 1977a. Raman spectroscopic investigation of the structure of silicate glasses: I. The binary alkali silicates. J. Phys. Chem. 63, 2421–2452.

Brawer, S.A., White, W.B., 1977b. Raman spectroscopic investigation of the structure of silicate glasses: II. Soda-alkaline earth-alumina ternary and quaternary glasses. J. Non-Cryst. Solids 23, 261–278.

Buchenau, U., Prager, M., Nücker, N., Dianoux, A.J., Ahmad, N., Phillips, W.A., 1986. Low-frequency modes in vitreous silica. Phys. Rev., B 34, 5665–5673.

Buckerman, W.-A., Müller-Warmuth, W., 1992. A further ^{29}Si NMR study on binary alkali silicate glasses. Glastech. Ber. 65, 18–21.

Clupper, D.C., Hench, L.L., 2003. Crystallization kinetics of tape cast bioactive glass 45S5. J. Non-Cryst. Solids 318, 43–48.

Cormack, A.N., Du, J., 2001. Molecular dynamics simulations of soda–lime silicate glasses. J. Non-Cryst. Solids 293–295, 283–289.

Cormier, L., Neuville, D.R., 2004. Ca and Na environments in Na_2O–CaO–Al_2O_3–SiO_2 glasses: influence of cation mixing and cation–network interactions. Chem. Geol. 213, 103–113.

Couette, M., 1888. La viscosité des liquides. Bull. Sci. Phys. 49, 123–262.

Couette, M., 1890. Etudes sur les frottements des liquides. Ann. Chim. Phys. 21, 433–496.

Davidon, W.C., 1966. Variable Metric Method for Minimization., pp., Argonne Natl. Lab. ANL 5990 3rd. revision, Lawrence Livermore.

English, S., 1923. The effect of composition on the viscosity of glass: Part II. J. Soc. Glass Technol. 8, 205–251.

Fontana, E.H., Plummer, W.A., 1979. A viscosity–temperature relation for glass. J. Am. Ceram. Soc. 62, 367–379.

Frantz, J.D., Mysen, B.O., 1995. Raman spectra and structure of BaO–SiO_2, SrO–SiO_2 and CaO–SiO_2 melts to 1600 °C. Chem. Geol. 121, 155–176.

Fukumi, K., Hayakawa, J., Komiyama, T., 1990. Intensity of Raman bands in silicate glasses. J. Non-Cryst. Solids 119, 297–302.

Furukawa, T., Fox, K.E., White, W.B., 1981. Raman spectroscopic investigation of the structure of silicate glasses: III. Raman intensities and structural units in soda silicate glasses. J. Chem. Phys. 153, 3226–3237.

Gehlgoff, G., Thomas, M., 1926. Die physikalischen eigenschaften der gläser in abhängigkeit von zusammensetzung: die viskosität der gläser. Z. Tech. Phys. 7, 260–278.

Hehlen, B., Courtens, E., Vacher, R., Yamanka, A., Kataoka, M., Inoue, K., 2000. Hyper-Raman scattering observation of the boson peak in vitreous silica. Phys. Rev. Lett. 84, 5355–5358.

Hehlen, B., Courtens, E., Yamanka, A., Inoue, K., 2002. Nature of the boson peak of silica glasses from hyper-Raman scattering. J. Non-Cryst. Solids 307, 185–190.

Hench, L.L., 1991. Bioceramics: from concept to clinic. J. Am. Ceram. Soc. 74, 1487–1510.

Jones, A.R., Winter, R., Greaves, G.N., Smith, I.H., 2001. MAS NMR study of soda–lime silicate glasses with variables degree of polymerisation. J. Non-Cryst. Solids 293–295, 87–92.

Kauzmann, W., 1948. The nature of the glassy state and the behavior of liquids at low temperatures. Chem. Rev. 43, 219–243.

Kim, H.-M., Miyaji, F., Kokubo, T., 1995. Bioactivity of Na_2O–CaO–SiO_2 glasses. J. Am. Ceram. Soc. 78, 2405–2411.

Kozyukov, V.M., Mazurin, O.V., 1994. Calculation of viscosity for soda lime silicate melts. Fiz. Khim. Stekla 20, 302–310.

Lazarev, A.N., 1972. Vibrational Spectra and Structure of Silicates. Consultants Bureau, New York.

Lee, S.K., 2005. Microscopic origins of macroscopic properties of silicate melts and glasses at ambient and high pressure: implications for melt generation and dynamics. Geochim. Cosmochim. Acta 69, 3695–3710.

Lee, S.K., Stebbins, J.F., 2003. Nature of cation mixing and ordering in Na–Ca silicate glasses and melts. J. Phys. Chem., B 107, 3141–3148.

Lejeune, A.M., Richet, P., 1995. Rheology of crystal-bearing silicate melts: an experimental study at high viscosity. J. Geophys. Res. 100, 4215–4229.

Lockyer, M.W.G., Holland, D., Dupree, R., 1995. NMR investigation of the structure of some bioactive and related glasses. J. Non-Cryst. Solids 188, 207–219.

Long, D.A., 1977. Raman Spectroscopy. McGraw-Hill, New York. 276 pp.

Maekawa, H., Maekawa, T., Kawamura, K., Yokokawa, T., 1991. The structural group of alkali silicate glasses determined from ^{29}Si MAS-NMR. J. Non-Cryst. Solids 127, 53–64.

Magnien, V., Neuville, D.R., Cormier, L., Mysen, B.O., Richet, P., 2004. Kinetics of iron oxidation in silicate melts: a preliminary XANES study. Chem. Geol. 213, 253–263.

Malinovsky, V.K., Sokolov, A.P., 1986. The nature of boson peak in Raman scattering in glasses. Solid State Commun. 57, 757–761.

Mastelaro, V.R., Zanotto, E.D., Lequeux, N., Cortes, R., 2000. Relationship between short-range order and ease of nucleation in $Na_2Ca_2Si_3O_9$, $CaSiO_3$ and $PbSiO_3$ glasses. J. Non-Cryst. Solids 262, 191–199.

Mazurin, O.V., Streltsina, M.V., Shvaiko-Shvaikovskaya, 1987. Handbook of Glass Date. Part C and B. Elsevier. 850 pp.

McMillan, P.F., 1984. A Raman spectroscopic study of glasses in the system $CaO–MgO–SiO_2$. Am. Mineral. 69, 645–659.

Meiling, G.S., Uhlmann, D.R., 1977. Crystallisation and melting kinetics of soda disilicate. Phys. Chem. Glasses 8, 62–68.

Morey, G.W., Bowen, N.L., 1925. The melting relations of the soda–lime–silica glasses. J. Soc. Glass Technol. 9, 226–264.

Mysen, B.O., 1988. Structure and Properties of Silicate Melts. Elsevier. 354 pp.

Mysen, B.O., 1990. The role of aluminum in depolymerized, peralkaline aluminosilicate melts in the systems $Li_2O–Al_2O_3–SiO_2$, $Na_2O–Al_2O_3–SiO_2$ and $K_2O–Al_2O_3–SiO_2$. Am. Mineral. 75, 120–134.

Mysen, B.O., Frantz, J.D., 1992. Structure and properties of alkali silicate melts at magmatic temperatures. Eur. J. Mineral. 5, 393–407.

Mysen, B.O., Frantz, J.D., 1994. Alkali silicate glass and melts structure in the temperature range 25–1651 °C at atmospheric pressure and implications for mixing behavior of structural units. Contrib. Mineral. Petrol. 117, 1–14.

Mysen, B.O., Richet, P., 2005. Silicate Glasses and Melts: Properties and Structure. Elsevier. 555 pp.

Mysen, B.O., Finger, L.W., Seifert, F.A., Virgo, D., 1982. Curve-fitting of Raman spectra of amorphous materials. Am. Mineral. 67, 686–696.

Napolitano, A., Hawkins, E.G., 1964. Viscosity of a standard soda–lime–silica glass. J. Res. NBS-A 68A, 439–448.

Neuville, D.R., 1992, Etude des propriétés thermodynamiques et rhéologiques des silicates fondus. Thesis, University of Paris VII. 350 pp.

Neuville, D.R., 2005. Structure and properties in (Sr, Na) silicate glasses and melts. Phys. Chem. Glasses 46, 112–118.

Neuville, D.R., Mysen, B.O., 1996. Role of aluminum in the silicate network: in situ, high-temperature study of glasses and melts on the joint $SiO_2–NaAlO_2$. Geochim. Cosmochim. Acta 60, 1727–1737.

Neuville, D.R., Richet, P., 1990. Viscosité et entropie des silicates fondues. Riv. Stn. Sper. Vetro 6, 213–220.

Neuville, D.R., Richet, P., 1991. Viscosity and (Ca,Mg) mixing in molten pyroxenes and garnets. Geochim. Cosmochim. Acta 55, 1011–1021.

Neuville, D.R., Courtial, P., Dingwell, D.B., Richet, P., 1993. Thermodynamic and rheological properties of rhyolite and andesite melts. Contrib. Mineral. Petrol. 113, 572–581.

Phillips, J.C., 1984. Microscopic origin of anomalously narrow Raman lines in network glasses. J. Non-Cryst. Solids 63, 347–355.

Poole, J.P., 1948. Viscosité à basse température des verres alcalino-silicatés. Verres Réfrac. 2, 222–230.

Richet, P., 1984. Viscosity and configurational entropy of silicate melts. Geochim. Cosmochim. Acta 48, 471–483.

Richet, P., 1987. Heat capacity of silicate glasses. Chem. Geol. 62, 111–124.

Richet, P., 2001. The Physical Basis of Thermodynamics: With Applications to Chemistry. Plenum Publisher. 442 pp.

Richet, P., Bottinga, Y., 1985. Heat capacity of aluminum-free liquid silicates. Geochim. Cosmochim. Acta 49, 471–486.

Richet, P., Bottinga, Y., 1995. Rheology and configurational entropy of silicate melts. Rev. Mineral. 32, 67–92.

Richet, P., Neuville, D.R., 1992. Thermodynamics of silicates melts: configurational properties. Adv. Phys. Geochem. 10, 132–161.

Richet, P., Robie, R.A., Hemingway, B.S., 1986. Low-temperature heat capacity of diopside glass ($CaMgSi_2O_6$): a calorimetric test of the configurational entropy theory applied to the viscosity of liquid silicates. Geochim. Cosmochim. Acta 50, 1521–1533.

Richet, P., Robie, R.A., Hemingway, B.S., 1993. Entropy and structure of silicates and melts. Geochim. Cosmochim. Acta 57, 2751–2766.

Richet, P., Bouhifd, M.A., Courtial, P., Téqui, C., 1997. Configurational heat capacity and entropy of borosilicate melts. J. Non-Cryst. Solids 211, 271–280.

Roling, B., Ingram, M.D., 2000. Mixed alkaline-earth effects in ion conducting glasses. J. Non-Cryst. Solids 265, 113–119.

Ryan, M., Blevins, S.1987. Viscosity of Silicate Melts and Glasses. U. S.G.S. 1764. 1080 pp.

Seifert, F.A., Mysen, B.O., Virgo, D., 1982. Three-dimensional network structure in the systems $SiO2–NaAlO_2$, $SiO_2–CaAl_2O_2$ and $SiO_2–MgAl_2O_2$. Am. Mineral. 67, 696–711.

Shartsis, L., Spinner, S., Capps, W., 1952. Density, expansivity and viscosity of molten alkali silicates. J. Am. Ceram. Soc. 35, 155–160.

Sipp, A., Neuville, D.R., Richet, P., 1997. Viscosity, configurational entropy and relaxation kinetics of borosilicate melts. J. Non-Cryst. Solids 211, 281–293.

Téqui, C., Robie, R.A., Hemingway, B.S., Neuville, D.R., Richet, P., 1991. Melting and thermodynamic properties of pyrope ($Mg_3Al_2Si_3O_{12}$). Geochim. Cosmochim. Acta 55, 1005–1011.

Toplis, M.J., 1998. Energy barriers to viscous flow and the prediction of glass transition temperature of molten silicates. Am. Mineral. 83, 480–490.

Vedishcheva, N.M., Shakhmatkin, B.A., Schultz, M.M., Vessal, B., Wright, A.C., Bachra, B., et al., 1995. A thermodynamic, molecular dynamics and neutron diffraction investigation of the tetrahedral {Si(n)} species and the network modifying cation environment in alkali silicate glasses. J. Non-Cryst. Solids 192 and 193, 292–297.

Wyckoff, R.W.G., Morey, G.W., 1925. X-ray diffraction measurements on some the soda–lime–silica glasses. J. Soc. Glass Technol. 9, 265–267.

Zotov, N., Keppler, H., 1998. The structure of sodium tetrasilicate glass from neutron diffraction, reverse Monte Carlo simulations and Raman spectroscopy. Phys. Chem. Miner. 25, 259–267.